ASM Sc. J., 12, Special Issue 5, 2019 for ICoAIMS2019, 17-25

Mixed Convective Stagnation Point Flow of a Thermally Stratified Hybrid Cu-Al_2O_3/Water Nanofluid over a Permeable Stretching/Shrinking Sheet

Najiyah Safwa Khashi'ie[1,2*], Norihan Md Arifin[1,3], Ezad Hafidz Hafidzuddin[4], Nadihah Wahi[3] and Ioan Pop[5]

[1]*Institute for Mathematical Research, Universiti Putra Malaysia, 43400 UPM Serdang, Selangor, Malaysia*

[2]*Fakulti Teknologi Kejuruteraan Mekanikal dan Pembuatan, Universiti Teknikal Malaysia Melaka, Hang Tuah Jaya, 76100 Durian Tunggal, Melaka, Malaysia*

[3]*Department of Mathematics, Faculty of Science, Universiti Putra Malaysia, 43400 UPM Serdang, Selangor, Malaysia*

[4]*Centre of Foundation Studies for Agricultural Science, Universiti Putra Malaysia, 43400 UPM Serdang, Selangor, Malaysia*

[5]*Department of Mathematics, Babeş-Bolyai University, R-400084 Cluj-Napoca, Romania*

The study scrutinizes the coupled effects of thermal stratification and mixed convection on boundary layer flow and heat transfer of a hybrid Cu-Al_2O_3/water nanofluid. Stretching/shrinking surface is permeable to allow the wall fluid suction while thermal convection is also included to deal with the thermal stratification phenomenon. In the present work, the combination of copper (Cu) nanoparticles and Al_2O_3/water nanofluid is modelled using the analytical hybrid nanofluid model. A similarity transformation is adopted to reduce the governing model into a set of ordinary (similarity) differential equations. The efficient boundary value problem with fourth order accuracy (bvp4c) solver in MATLAB software is utilized to solve the transformed model. An astonishing result is obtained where the heat transfer rate of hybrid nanofluid intensifies when small suction parameter is imposed on the stretching/shrinking sheet while a contrary result is obtained when higher value of suction is applied. Suction and opposing buoyancy parameters are among the control parameters that induce the existence of second solution. Stability analysis affirms that the first solution is mathematically stable. The present results are conclusive to the combination of alumina and copper nanoparticles only and other combination of nanoparticles may produce different flow and heat transfer characteristics.

Keywords: stagnation point flow; hybrid nanofluid; stretching/shrinking; thermal stratification; dual solutions

I. INTRODUCTION

Nanoparticles are a nano-sized solid particle (<100nm) which are effectively used in the invention of traditional nanofluid to optimize the thermal conductivity of conventional coolants or base fluids (i.e. ethylene glycol, water, mixture of water and ethylene glycol, vegetable oil or transformer oil). There are a few types of nanoparticles that are widely used; metal oxides (i.e. alumina/Al_2O_3, hematite/Fe_2O_3, magnetite/Fe_3O_4, cupric oxide/CuO), metals (copper/Cu, silver/Ag), metal carbide and carbon materials (i.e. carbon nanotube/CNT, multi-walled carbon nanotubes/MWCNT, graphite). Further, hybrid nanofluid is an extension of traditional nanofluid, which is prepared by dispersing different nanoparticles in a base fluid. The evolution of stable hybrid nanofluids may lead to the energy sustainability since it can enhance the thermal system efficiency (Das, 2017). A few of literatures had reported on the preparation, thermal conductivity and

Corresponding author's e-mail: najiyah@utem.edu.my

recent applications of the hybrid nanofluids (Jana *et al.*, 2007; Sarkar *et al.*, 2015; Sidik *et al.*, 2016; Sundar *et al.*, 2017; Babu *et al.*, 2017; Sajid & Ali, 2018; Gupta *et al.*, 2018; Huminic & Huminic, 2018). According to (Suresh *et al.*, 2011), alumina has low thermal conductivity as compared to the copper nanoparticles, but the good side is alumina has well stability and chemical inaction. The combination of least amounts of copper solid volume fraction into an alumina matrix could maintain the stability of hybrid nanofluid and substantially, boost the thermal properties.

(Devi & Devi, 2016) introduced a new special form of thermophysical properties to solve the boundary layer problem for hybrid nanofluid model. These properties were compared with the experimental results for the model authentication and applied into the (Tiwari & Das, 2007) model of nanofluid. (Nadeem *et al.*, 2018) analyzed the thermal slip effect on stagnation point flow of a hybrid Cu-Al_2O_3/water nanofluid past a circular cylinder while (Yousefi *et al.*, 2018) analyzed the combined effects of titania and copper towards a wavy cylinder. (Rostami *et al.*, 2018) solved the mixed convective stagnation point flow of a silica-alumina/water hybrid nanofluid and obtained dual solutions. (Dinarvand, 2019) utilized hybrid CuO-Ag/water nanofluid model and investigated the nodal/saddle stagnation point flow.

Inspired by the previous literatures, the present work accentuates the stagnation point flow of a hybrid Cu-Al_2O_3/water nanofluid over a permeable stretching/shrinking sheet with thermal stratification effect. The authors also concern the emergence of non-unique solution in the present problem and how the stability analysis is formulated and conducted to verify the reliability of the solutions.

II. PROBLEM FORMULATION

Consider a laminar, steady and incompressible stagnation point flow of a hybrid nanofluid due to a permeable stretching/shrinking sheet with linear velocity $u_w(x) = ax/L$ as depicted in Figure 1. The free stream velocity is assumed as $u_e(x) = bx/L$, with b is a positive constant. A few of presumptions are also examined for the physical model:

- The base fluid and nanoparticles are maintained in a thermal equilibrium state.
- The spherical shaped nanoparticles are considered with uniform size.
- The sheet is permeable to allow the fluid suction/injection process.
- Thermal buoyancy force is considered to deal with the thermal stratification phenomenon (Mat Yasin *et al.* 2013; Besthapu *et al.* 2017; Animasaun *et al.* 2019).
- The linear stratified ambient temperature is $T_\infty(x) = T_0 + A(x/L)$; T_0 is the initial ambient temperature of the hybrid nanofluid, L is the characteristic length of the sheet and A is a constant.
- The wall temperature is $T_w(x) = T_0 + B(x/L)$; $T_w(x) > T_\infty(x)$ specified for a heated sheet (assisting flow) while $T_w(x) < T_\infty(x)$ specified for a cooled sheet (opposing flow).

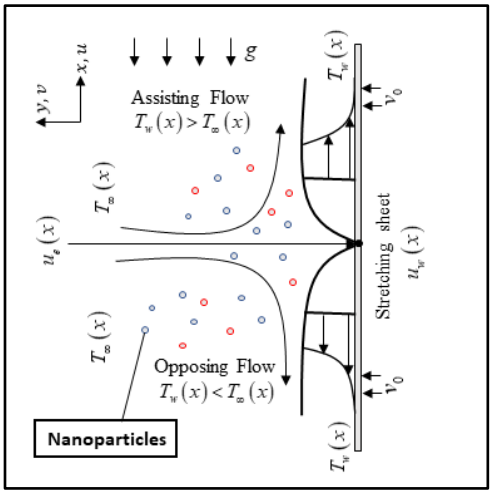

(a)

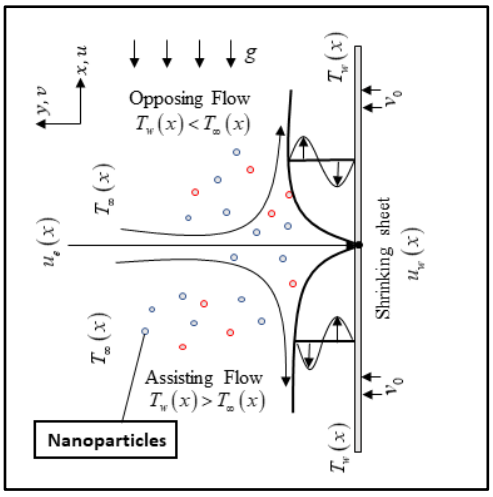

(b)

Figure 1. The physical model of mixed convective stagnation point flow over (a) stretching (b) shrinking surface.

Under all these assumptions, the governing boundary layer equations are:

$$\frac{\partial u}{\partial x}+\frac{\partial v}{\partial y}=0, \tag{1}$$

$$u\frac{\partial u}{\partial x}+v\frac{\partial u}{\partial y}=u_e\frac{du_e}{dx}+\frac{\mu_{hnf}}{\rho_{hnf}}\frac{\partial^2 u}{\partial y^2}+\frac{g\left(\rho\beta_T\right)_{hnf}\left(T-T_\infty\right)}{\rho_{hnf}}, \tag{2}$$

$$u\frac{\partial T}{\partial x}+v\frac{\partial T}{\partial y}=\left(\frac{k}{\rho C_p}\right)_{hnf}\frac{\partial^2 T}{\partial y^2}, \tag{3}$$

subject to the boundary conditions

$$\begin{aligned} &u(x,0)=u_w(x),\quad v(x,0)=v_0,\quad T(x,0)=T_w(x),\\ &u(x,y)\to u_e(x),\quad T(x,y)\to T_\infty(x),\quad \text{as}\quad y\to\infty. \end{aligned} \tag{4}$$

Here u and v are the velocity components along x and $y-$ directions, accordingly, T is the fluid temperature, ν_f is the kinematic viscosity of the base fluid, $v_0=-S\sqrt{b\nu_f}$ is the constant mass flow with $v_0<0$ and $v_0>0$ are for suction and injection, respectively.

Table 1 correlates the thermophysical properties between hybrid and traditional nanofluids where ρ, ρC_p, μ, k and β_T are the term for the density, heat capacity, dynamic viscosity, thermal conductivity and thermal expansion, correspondingly. The subscripts hnf, nf, f, $s1$ and $s2$ indicate the hybrid nanofluid, nanofluid, base fluid, first and second nanoparticles, mutually. It is also noted that ϕ represents the nanoparticles volume fraction (ϕ_1 for first nanoparticle and ϕ_2 for second nanoparticle). The thermophysical properties of the alumina (Al_2O_3) and copper (Cu) nanoparticles with base fluid (water) are exemplified in Table 2.

In the present work, a set of similarity transformations (see Equation (5)) is adopted

$$\begin{aligned} &u=u_e(x)f'(\eta),\quad v=-\sqrt{\frac{u_e(x)\nu_f}{x}}f(\eta),\\ &\theta(\eta)=\frac{T-T_\infty(x)}{T_w(x)-T_0},\quad \eta=y\sqrt{\frac{u_e(x)}{x\nu_f}}, \end{aligned} \tag{5}$$

to the Equations (2) and (3) and subsequently, the following ODEs are obtained:

$$\left(\frac{\mu_{hnf}/\mu_f}{\rho_{hnf}/\rho_f}\right)f'''+ff''-f'^2+1+A_1\lambda\theta=0, \tag{6}$$

$$\frac{1}{\Pr}\frac{k_{hnf}/k_f}{\left(\rho C_p\right)_{hnf}/\left(\rho C_p\right)_f}\theta''+f\theta'-\left(\theta+\delta\right)f'=0, \tag{7}$$

inclusive of the boundary conditions:

$$\begin{aligned} &f(0)=S,\quad f'(0)=\varepsilon,\quad \theta(0)=1-\delta,\\ &f'(\eta)\to 1,\quad \theta(\eta)\to 0,\quad \text{as}\quad \eta\to\infty \end{aligned} \tag{8}$$

Table 1. The thermophysical properties between hybrid and traditional nanofluid

Properties	Hybrid Nanofluid	Traditional Nanofluid
Density	$\rho_{hnf}=(1-\phi_2)\left[(1-\phi_1)\rho_f+\phi_1\rho_{s1}\right]+\phi_2\rho_{s2}$	$\rho_{nf}=(1-\phi)\rho_f+\phi\rho_s$
Heat Capacity	$\left(\rho C_p\right)_{hnf}=(1-\phi_2)\left[(1-\phi_1)\left(\rho c_p\right)_f+\phi_1\left(\rho c_p\right)_{s1}\right]+\phi_2\left(\rho c_p\right)_{s2}$	$\left(\rho C_p\right)_{nf}=(1-\phi)\left(\rho c_p\right)_f+\phi\left(\rho c_p\right)_s$
Dynamic Viscocity	$\frac{\mu_{hnf}}{\mu_f}=\frac{1}{(1-\phi_1)^{2.5}(1-\phi_2)^{2.5}}$	$\frac{\mu_{nf}}{\mu_f}=\frac{1}{(1-\phi_1)^{2.5}}$
Thermal Conductivity	$\frac{k_{hnf}}{k_{bf}}=\left[\frac{k_{s2}+2k_{bf}-2\phi_2\left(k_{bf}-k_{s2}\right)}{k_{s2}+2k_{bf}+\phi_2\left(k_{bf}-k_{s2}\right)}\right]$ where $\frac{k_{bf}}{k_f}=\left[\frac{k_{s1}+2k_f-2\phi_1\left(k_f-k_{s1}\right)}{k_{s1}+2k_f+\phi_1\left(k_f-k_{s1}\right)}\right]$	$\frac{k_{nf}}{k_f}=\left[\frac{k_s+2k_f-2\phi\left(k_f-k_s\right)}{k_s+2k_f+\phi\left(k_f-k_s\right)}\right]$
Thermal Expansion	$\left(\rho\beta_T\right)_{hnf}=(1-\phi_2)\left[(1-\phi_1)\left(\rho\beta_T\right)_f+\phi_1\left(\rho\beta_T\right)_{s1}\right]+\phi_2\left(\rho\beta_T\right)_{s2}$	$\left(\rho\beta_T\right)_{nf}=(1-\phi)\left(\rho\beta_T\right)_f+\phi\left(\rho\beta_T\right)_s$

Table 2. Thermophysical properties of the alumina, copper and water (see Rostami *et al.*)

Physical properties	$\rho\left(\mathrm{kg/m^3}\right)$	$C_p\left(\mathrm{J/kgK}\right)$	$k\left(\mathrm{W/mK}\right)$	$\beta_T\times10^5\left(\mathrm{K^{-1}}\right)$
Alumina	3970	765	40	0.85
Copper	8933	385	400	1.67
Water	997.1	4179	0.6130	21

where $\lambda = Gr/\mathrm{Re}_x^{\,2}$ is the buoyancy parameter, $Gr = g(\beta_T)_f (T_w(x) - T_0)x^3/\nu_f^{\,2}$ is the Grashof number, $A_1 = \dfrac{(1-\phi_2)\left[(1-\phi_1)\rho_f + \phi_1(\rho\beta_T)_{s1}/(\beta_T)_f\right] + \phi_2(\rho\beta_T)_{s2}/(\beta_T)_f}{(1-\phi_2)\left[(1-\phi_1)\rho_f + \phi_1\rho_{s1}\right] + \phi_2\rho_{s2}}$, $\mathrm{Re}_x = xu_e(x)/\nu_f$ is the local Reynolds number. It also worth to mention that $\lambda > 0$ corresponds to the assisting flow, $\lambda < 0$ for the opposing flow and $\lambda = 0$ for the forced convection flow. Additionally, $\mathrm{Pr} = (C_p\mu)_f/k_f$ is the Prandtl number, S is the wall mass suction/injection parameter, $\varepsilon = a/b$ is the velocity ratio parameter ($\varepsilon > 0$ for stretching sheet, $\varepsilon < 0$ for shrinking sheet and $\varepsilon = 0$ is for static sheet) and $\delta = A/B$ is the thermal stratification parameter.

The skin friction coefficient C_f and the local Nusselt number Nu_x, are described as

$$C_f = \frac{\tau_w}{\rho_f u_e^2}, \qquad Nu_x = \frac{xq_w}{k_f(T_w(x) - T_0)}, \tag{9}$$

where τ_w is the surface shear stress and q_w is the surface heat flux, which are defined as

$$\tau_w = \mu_{hnf}\left(\frac{\partial u}{\partial y}\right)_{y=0}, \qquad q_w = -k_{hnf}\left(\frac{\partial T}{\partial y}\right)_{y=0}. \tag{10}$$

Using (5), (9) and (10), the following reduced skin friction coefficient and heat transfer rate are attained

$$\mathrm{Re}_x^{1/2} C_f = \frac{\mu_{hnf}}{\mu_f} f''(0), \qquad \mathrm{Re}_x^{-1/2} Nu_x = -\frac{k_{hnf}}{k_f}\theta'(0). \tag{11}$$

III. STABILITY ANALYSIS

There are a few of literatures that discussed the significance and full formulation of the stability analysis (Ismail *et al.* 2016; Jamaludin *et al.* 2019; Khashi'ie *et al.* 2019; Khashi'ie *et al.* 2019). First step in the stability process is to consider the unsteady form of Equations (2) and (3):

$$\frac{\partial u}{\partial t} + u\frac{\partial u}{\partial x} + v\frac{\partial u}{\partial y} = u_e\frac{du_e}{dx} + \frac{\mu_{hnf}}{\rho_{hnf}}\frac{\partial^2 u}{\partial y^2} + \frac{g(\rho\beta_T)_{hnf}(T - T_\infty)}{\rho_{hnf}}, \tag{12}$$

$$\frac{\partial T}{\partial t} + u\frac{\partial T}{\partial x} + v\frac{\partial T}{\partial y} = \left(\frac{k}{\rho C_p}\right)_{hnf}\frac{\partial^2 T}{\partial y^2}. \tag{13}$$

A new set of transformations (see Equation (14)) with dimensionless time variable τ is introduced and applied to Equations (12) and (13):

$$u = u_e(x) f'(\eta,\tau), \quad v = -\sqrt{\frac{u_e(x)\nu_f}{x}} f(\eta,\tau),$$
$$\theta(\eta,\tau) = \frac{T - T_\infty(x)}{T_w(x) - T_0}, \quad \eta = y\sqrt{\frac{u_e(x)}{x\nu_f}}, \quad \tau = bt. \tag{14}$$

The new transformed nonlinear differential equations are:

$$\frac{\mu_{hnf}/\mu_f}{\rho_{hnf}/\rho_f}\frac{\partial^3 f}{\partial\eta^3} + f\frac{\partial^2 f}{\partial\eta^2} - \left(\frac{\partial f}{\partial\eta}\right)^2 + 1 + A_1\lambda\theta - \frac{\partial^2 f}{\partial\eta\partial\tau} = 0, \tag{15}$$

$$\frac{1}{\mathrm{Pr}}\frac{k_{hnf}/k_f}{(\rho C_p)_{hnf}/(\rho C_p)_f}\frac{\partial^2\theta}{\partial\eta^2} + f\frac{\partial\theta}{\partial\eta} - (\theta + \delta)\frac{\partial f}{\partial\eta} - \frac{\partial\theta}{\partial\tau} = 0, \tag{16}$$

with the conditions

$$\begin{aligned} &f(0,\tau) = S, \quad \frac{\partial f}{\partial\eta}(0,\tau) = \varepsilon, \quad \theta(0,\tau) = 1 - \delta, \\ &\frac{\partial f}{\partial\eta}(\eta,\tau) \to 1, \quad \theta(\eta,\tau) \to 0, \quad \text{as} \quad \eta \to \infty. \end{aligned} \tag{17}$$

Further, the following expressions are tested into Equations (15)-(17) to validate the reliability of the steady flow solutions $f(\eta) = f_0(\eta)$ and $\theta(\eta) = \theta_0(\eta)$. In the formulation, γ is an unidentified eigenvalue whereas $F(\eta)$ and $G(\eta)$ are a small relative to $f_0(\eta)$ and $\theta_0(\eta)$, respectively.

$$\left.\begin{aligned} f(\eta,\tau) &= f_0(\eta) + e^{-\gamma\tau}F(\eta), \\ \theta(\eta,\tau) &= \theta_0(\eta) + e^{-\gamma\tau}G(\eta), \end{aligned}\right\} \tag{18}$$

The linearized eigenvalue problem is produced by adopting Equation (18) into Equations (15)-(17)

$$\frac{\mu_{hnf}/\mu_f}{\rho_{hnf}/\rho_f}F''' + Ff_0'' + f_0F'' - \left(2f_0' - \gamma\right)F' + A_1\lambda G = 0, \tag{19}$$

$$\begin{aligned} &\frac{1}{\mathrm{Pr}}\frac{k_{hnf}/k_f}{(\rho C_p)_{hnf}/(\rho C_p)_f}G'' + F\theta_0' + f_0G' - (\theta_0 + \delta)F' \\ &-\left(f_0' - \gamma\right)G = 0, \end{aligned} \tag{20}$$

in conjunction with

$$\left.\begin{aligned} &F(0) = F'(0) = G(0) = 0, \\ &F'(\infty) \to 0, \quad G(\infty) \to 0, \end{aligned}\right\} \tag{21}$$

In the bvp4c solver, Equations (19)-(21) are computed to find the possible range of eigenvalues. The sign of the smallest eigenvalue (γ_1) will act as a determinant of the real solution; positive γ_1 indicates that the solution is stable/real while negative γ_1 signifies that the solution is unstable. However, to make it happen, one of the boundary

conditions $\left(F'(\infty)\to 0 \text{ or } G(\infty)\to 0\right)$ need to be substituted with a new relaxing condition. In the present work, $F'(\infty)\to 0$ in Equation (21) is replaced with a new boundary condition $F''(0)=1$.

IV. RESULT AND DISCUSSION

The ordinary (similarity) differential equations are successfully computed for selected values of the pertinent parameters; suction S, velocity ratio ε, thermal buoyancy λ, thermal stratification δ, and nanoparticles solid volume fraction (ϕ_1,ϕ_2) using the bvp4c package in MATLAB software. The bvp4c function was programmed with a finite difference Lobatto IIIa scheme (three-stage) with fourth order accuracy. The main objectives in the present work are (a) to study the impact of selected physical parameters on the dimensionless velocity and temperature profiles as well as the skin friction coefficient and heat transfer rate, and (b) to identify all the possible solution(s) that may arise in the governing problem. Existing literatures had proved that the dual and multiple solutions were possible for the shrinking flow case with suction, thermal buoyancy or stagnation region. $\Pr=6.2$ is fixed in the entire study to symbolize water as the base fluid. Further, following the works by (Devi & Devi, 2016) and (Nadeem *et al.*, 2018), the first nanoparticle (ϕ_1) is alumina with 10% solid volume fraction whereas the solid volume fraction for second nanoparticle (copper) is varied $1\%\le\phi_1\le 5\%$. The combination of both nanoparticles with pure water as the base fluid will generate a hybrid Cu-Al_2O_3/water nanofluid model while Cu-water and Al_2O_3-water nanofluids are created when $\phi_1=0$ or $\phi_2=0$, respectively. The model is reduced to the viscous/Newtonian fluid when both $\phi_1=\phi_2=0$.

Tables 3 and 4 correlate the values of $f''(0)$ and $-\theta'(0)$ between present result and those by (Rostami *et al.*, 2018) and (Ishak *et al.*, 2010) when all the physical parameters are zero except $\lambda=1$. (Rostami *et al.*, 2018) adopted the bvp4c solver to compute the mixed convective stagnation point flow of hybrid nanofluid while (Ishak *et al.*, 2010) applied the Keller-box method to study the mixed convective stagnation point flow of viscous fluid. Both literatures considered a permeable flat plate $(\varepsilon=0)$ in their work. The approximate percent relative error $\left(\varepsilon_a=\left|(a-b)/a\right|\times 100\%\right)$ is also calculated to compare the present result, a and previous result, b. It shows that ε_a between present and previous results are sufficiently small $(0\%\le\varepsilon_a<0.5\%)$, thus the bvp4c method used in the present work is accepted and well-used.

Table 3. A comparison of $f''(0)$ when $S=\varepsilon=\delta=0$ and $\lambda=1$ for viscous fluid ($\phi_1=\phi_2=0$)

Pr	Present (bvp4c)		(Rostami *et al.*, 2018) (bvp4c)				(Ishak *et al.*, 2010) (Keller-box)			
	First Solution	Second Solution	First Solution	ε_a (%)	Second Solution	ε_a (%)	First Solution	ε_a (%)	Second Solution	ε_a (%)
0.7	1.7063	1.2387	1.7063	0	1.2344	0.35	1.7063	0	1.2387	0
1	1.6754	1.1332	1.6754	0	1.1296	0.32	1.6754	0	1.1332	0
7	1.5179	0.5824	1.5179	0	0.5815	0.15	1.5179	0	0.5824	0

Table 4. A comparison of $-\theta'(0)$ when $S=\varepsilon=\delta=0$ and $\lambda=1$ for viscous fluid ($\phi_1=\phi_2=0$)

Pr	Present (bvp4c)		(Rostami *et al.*, 2018) (bvp4c)				(Ishak *et al.*, 2010) (Keller-box)			
	First Solution	Second Solution	First Solution	ε_a (%)	Second Solution	ε_a (%)	First Solution	ε_a (%)	Second Solution	ε_a (%)
0.7	0.7641	1.0226	0.7641	0	1.0235	0.09	0.7641	0	1.0226	0
1	0.8708	1.1691	0.8708	0	1.1706	0.13	0.8708	0	1.1691	0
7	1.7224	2.2192	1.7224	0	2.2203	0.05	1.7224	0	2.2192	0

Figure 2 exemplifies $\mathrm{Re}_x^{1/2}C_f$ and $\mathrm{Re}_x^{-1/2}Nu_x$ towards S when $\phi_2=0.01$, 0.03 and 0.05. It is noticed that dual solutions are possible in the study for the shrinking case $(\varepsilon=-1)$ if $S\ge S_c$ and unique/distinctive solution is obtained when

$S = S_c$. The boundary layer starts separating (laminar to turbulent) when $S < S_c$ and at this stage the full Navier-Stokes with Fourier energy model are used to observe the flow characteristics. Suction is one of the control parameters that is necessary in the present work to induce two (non-unique) solutions while the application of injection parameter $(S < 0)$ will not generate any similarity solution. Figure 2 also portrays that both skin friction coefficient and heat transfer rate for first solution incline with the increment of the ϕ_2. However, this observation is only valid for $S \le 1$ and the flow characteristics may differ for $S > 1$ as clarified in Figure 3. A comparison of $\mathrm{Re}_x^{-1/2} Nu_x$ between viscous fluid, Cu-water nanofluid $(\phi_1 = 0,\ \phi_2 = 0.01)$ and Cu-Al_2O_3/water hybrid nanofluid $(\phi_1 = 0.1,\ \phi_2 = \text{varied})$ is manifested in Figure 3 when $S = 0.5$ and $S = 2$. Hybrid nanofluid with 5% solid volume fraction of copper has higher heat transfer rate as compared to the traditional nanofluid and viscous fluid when $S = 0.5$ for both stretching and shrinking cases. However, astonishing result is achieved when higher S $(S = 2)$ is applied. The value of $\mathrm{Re}_x^{-1/2} Nu_x$ for viscous fluid is greater as compared to the traditional and hybrid nanofluids. Nevertheless, it is obvious from the stretching case that the heat transfer rate of hybrid nanofluid is slightly intensified as ϕ_2 enhances.

The $\mathrm{Re}_x^{1/2} C_f$ and $\mathrm{Re}_x^{-1/2} Nu_x$ towards λ when $S = 0.5,\ 0.6$ and 0.7 is graphically manifested in Figure 4. It indicates that the thermal buoyancy parameter (opposing flow) also can lead to dual solutions. However, no second solution is obtained when $\lambda = 0$ (forced convection flow) while higher value of suction conceivably desired to generate two solution in the assisting flow region. It can be seen when $S = 0.5$, the second solution in assisting flow region, can only sustain for approximately $0 < \lambda < 0.8$. Figure 4 also reveals that the skin friction coefficient and heat transfer rate for the first solution escalates when S is enhanced for all types of convective flow (free and forced).

Figures 5 and 6 elucidate the velocity and temperature profiles for both stretching flow $(\varepsilon = 0.5)$ and shrinking flow $(\varepsilon = -1)$ cases when ϕ_2 is enhanced. There is only a slight accretion for both velocity and temperature profiles of the first solution whereas a contrary result is noticed for the second solution. The boost of nanoparticles solid volume fraction generally may develop more energies and subsequently, increase the temperature profile. Nevertheless, the profiles of second solution are not in accordance with the theoretical judgment. Hence, the stability analysis in the previous section is used to justify the real solution between first and second solutions. It also worth to mention that the results in Figures 5 and 6 only applicable for assisting buoyancy parameter $(\lambda = 0.5)$ and the usage of opposing buoyancy parameter may produce different flow characteristics.

A stability analysis is conducted by solving the linearized eigenvalue problem in Equations (19)-(21) using bvp4c solver in MATLAB software. Figure 7 demonstrates the smallest eigenvalue γ_1 towards thermal buoyancy parameter λ for both first and second solutions. It shows that the first and second solutions hold positive and negative γ_1, correspondingly and $\gamma_1 \to 0$ as $\lambda \to \lambda_c$. This result mathematically supports and validates that the first solution is the real solution.

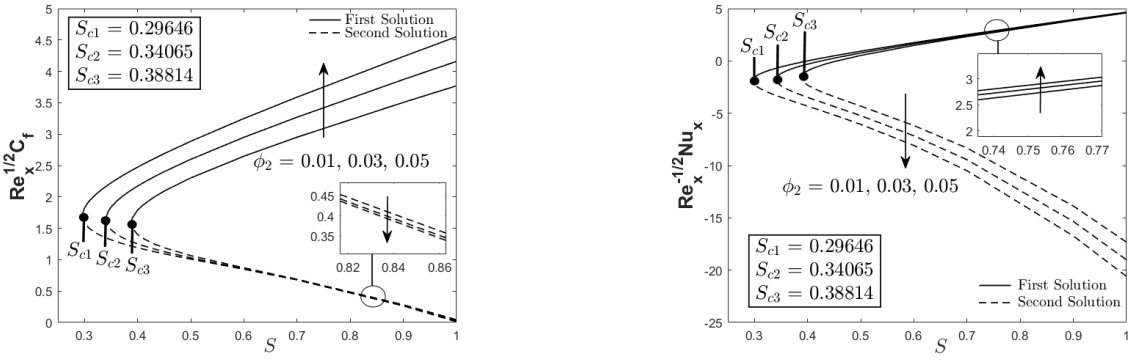

(a) (b)

Figure 2. (a) $\mathrm{Re}_x^{1/2} C_f$ (b) $\mathrm{Re}_x^{-1/2} Nu_x$ towards S when $\delta = 0.01,\ \lambda = -1$ and $\varepsilon = -1$

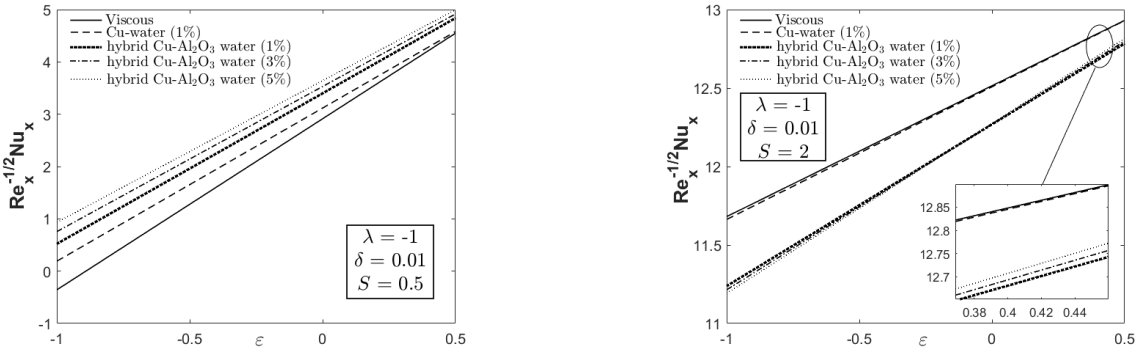

(a) (b)

Figure 3. $\mathrm{Re}_x^{-1/2} Nu_x$ towards ε when (a) $S = 0.5$ (b) $S = 2$

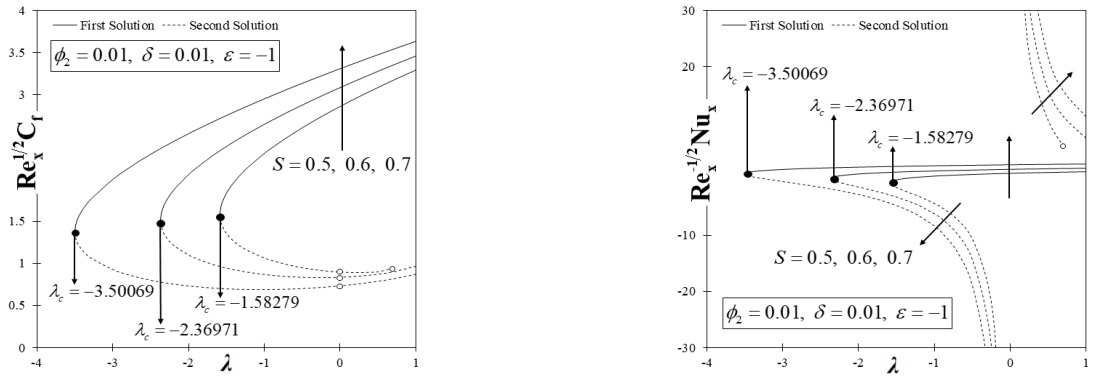

(a) (b)

Figure 4. (a) Skin friction coefficient (b) Heat transfer rate towards λ for different values of S

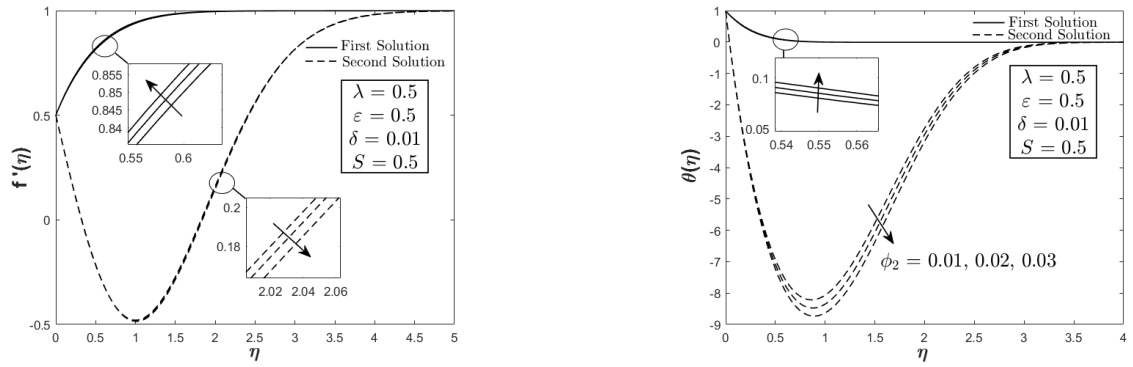

(a) (b)

Figure 5. (a) Velocity (b) Temperature profiles for stretching flow case when $\phi_2 = 0.01, 0.02$ and 0.03

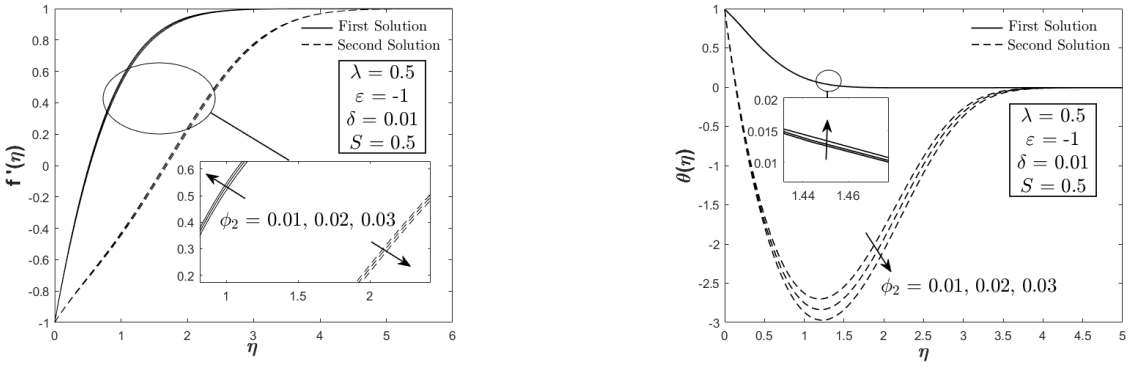

(a) (b)

Figure 6. (a) Velocity (b) Temperature profiles for shrinking flow case when $\phi_2 = 0.01, 0.02$ and 0.03

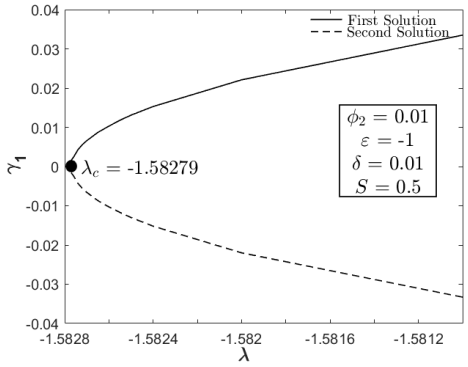

Figure 7. The smallest eigenvalue γ_1 towards thermal buoyancy parameter λ for both first and second solutions

V. CONCLUSION

The present work highlights the mixed convective stagnation point flow of a thermally stratified hybrid Cu-Al_2O_3/water nanofluid over a permeable stretching/shrinking sheet. The variable wall temperature and linear stratified form of ambient temperature are considered. The similarity solution is successfully computed using the efficient bvp4c solver in the MATLAB software. The conclusions are as follows:

- Two solutions (first and second) are possible in the present investigation within a certain range of the suction parameter S and thermal buoyancy parameter λ.
- The stability analysis affirms that the first solution is the real solution. In addition, the second solution is mathematically and physically (graph observation) validated as unstable solution.
- The hybrid Cu-Al_2O_3/water nanofluid has greater heat transfer rate as compared to the Cu-water nanofluid and viscous (water) fluid when $S = 0.5$ is enhanced to the shrinking sheet. Surprisingly, opposite result is obtained when $S = 2$ is applied to the shrinking sheet.
- This study may provide idea to the other researchers on how to increase/decrease the heat transfer rate (depends on the engineering and technological demands) by controlling parameters such as suction, copper nanoparticles volume fraction or buoyancy.
- The present result is decisive to the combination of alumina and copper nanoparticles only.

VI. ACKNOWLEDGEMENT

The authors would like to acknowledge Universiti Putra Malaysia through the financial support via Putra Grant-9570600. The support from Ministry of Education (Malaysia) and Universiti Teknikal Malaysia Melaka UTEM-SLAB scholarship also gratefully appreciated.

VII. REFEREENCES

Animasaun, IL, Makinde, OD & Saleem, S 2019, 'Mixed convection flow of Newtonian fluids over an upper horizontal thermally stratified melting surface of a paraboloid of revolution', *Journal of the Brazilian Society of Mechanical Sciences and Engineering*, vol. *41,* no. 4, pp. 197.

Babu, JR, Kumar, KK & Rao, SS 2017, 'State-of-art review on hybrid nanofluids', *Renewable and Sustainable Energy Reviews*, vol. *77*, pp. 551-565.

Besthapu, P, Haq, RU, Bandari, S & Al-Mdallal, QM 2017, 'Mixed convection flow of thermally stratified MHD nanofluid over an exponentially stretching surface with viscous dissipation effect', *Journal of the Taiwan Institute of Chemical Engineers*, vol. *71*, pp. 307-314.

Das, PK 2017, 'A review based on the effect and mechanism of thermal conductivity of normal nanofluids and hybrid nanofluids', *Journal of Molecular Liquids*, vol. *240*, pp. 420-446.

Devi, SA & Devi, SSU 2016, 'Numerical investigation of hydromagnetic hybrid Cu–Al_2O_3/water nanofluid flow over a permeable stretching sheet with suction', *International Journal of Nonlinear Sciences and Numerical Simulation*, vol. *17, no.* 5, pp. 249-257.

Dinarvand, S 2019, 'Nodal/saddle stagnation-point boundary layer flow of CuO–Ag/water hybrid nanofluid: a novel hybridity model', *Microsystem Technologies*, vol. 25, no. 7, pp. 2609-2623.

Gupta, M, Singh, V, Kumar, S, Kumar, S, Dilbaghi, N & Said, Z 2018, 'Up to date review on the synthesis and thermophysical properties of hybrid nanofluids', *Journal of cleaner production*, vol. *190*, pp. 169-192.

Huminic, G & Huminic, A 2018, 'Hybrid nanofluids for heat transfer applications–A state-of-the-art review', *International Journal of Heat and Mass Transfer*, vol. *125*, pp. 82-103.

Ishak, A, Nazar, R, Bachok, N & Pop, I 2010, 'MHD mixed

convection flow near the stagnation-point on a vertical permeable surface', *Physica A: Statistical Mechanics and its Applications*, no. *389*, vol. 1, pp. 40-46.

Ismail, NS, Arifin, NM, Nazar, R, Bachok, N & Mahiddin, N 2016, 'Stability analysis in stagnation-point flow towards a shrinking sheet with homogeneous–Heterogeneous reactions and suction effects', *International Journal of Applied Engineering Research*, vol. *11*, no. 18, pp. 9229-9235.

Jamaludin, A, Nazar, R & Pop, I 2019, 'Mixed convection stagnation-point flow of a nanofluid past a permeable stretching/shrinking sheet in the presence of thermal radiation and heat source/sink', *Energies*, vol. *12,* no. 5, pp. 788.

Jana, S, Salehi-Khojin, A & Zhong, WH 2007, 'Enhancement of fluid thermal conductivity by the addition of single and hybrid nano-additives', *Thermochimica acta*, vol. *462*, no. 1-2, pp. 45-55.

Khashi'ie, NS, Arifin, NM, Hafidzuddin, EH & Wahi, N 2019, 'MHD Mixed Convective Stagnation Point Flow with Heat Generation Past a Shrinking Sheet', *ASM Science Journal*, vol. *12*, Special Issue 1, pp. 71-81.

Khashi'ie, NS, Arifin, NM, Nazar, R, Hafidzuddin, EH, Wahi, N & Pop, I 2019, 'A Stability Analysis for Magnetohydrodynamics Stagnation Point Flow with Zero Nanoparticles Flux Condition and Anisotropic Slip', *Energies*, vol. *12*, no. 7, pp. 1268.

Mat Yasin, MH, Arifin, NM, Nazar, R, Ismail, F & Pop, I 2013, 'Mixed Convection Boundary Layer Flow Embedded in a Thermally Stratified Porous Medium Saturated by a Nanofluid', *Advances in Mechanical Engineering*, vol. *5*, pp. 121943.

Nadeem, S, Abbas, N & Khan, AU 2018, 'Characteristics of three dimensional stagnation point flow of Hybrid nanofluid past a circular cylinder', *Results in physics*, vol. *8*, pp. 829-835.

Rostami, MN, Dinarvand, S & Pop, I 2018, 'Dual solutions for mixed convective stagnation-point flow of an aqueous silica–alumina hybrid nanofluid', *Chinese Journal of Physics*, vol. *56,* no. 5, pp. 2465-2478.

Sajid, MU & Ali, HM 2018, 'Thermal conductivity of hybrid nanofluids: a critical review', *International Journal of Heat and Mass Transfer*, vol. *126*, pp. 211-234.

Sarkar, J, Ghosh, P & Adil A 2015, 'A review on hybrid nanofluids: recent research, development and applications', *Renewable and Sustainable Energy Reviews*, vol. *43*, pp. 164-177.

Sidik, NAC, Adamu, IM, Jamil, MM, Kefayati, GHR, Mamat, R & Najafi, G 2016, 'Recent progress on hybrid nanofluids in heat transfer applications: a comprehensive review', *International Communications in Heat and Mass Transfer*, vol. *78*, pp. 68-79.

Sundar, LS, Sharma, KV, Singh, MK & Sousa, ACM 2017, 'Hybrid nanofluids preparation, thermal properties, heat transfer and friction factor–a review', *Renewable and Sustainable Energy Reviews*, vol. *68*, pp. 185-198.

Suresh, S, Venkitaraj, KP, Selvakumar, P & Chandrasekar, M 2011, 'Synthesis of Al_2O_3–Cu/water hybrid nanofluids using two step method and its thermo physical properties', *Colloids and Surfaces A: Physicochemical and Engineering Aspects*, vol. *388,* no. 1-3, pp. 41-48.

Tiwari, RK & Das, MK 2007, 'Heat transfer augmentation in a two-sided lid-driven differentially heated square cavity utilizing nanofluids', *International Journal of heat and Mass transfer*, vol. *50*, no. 9-10, pp. 2002-2018.

Yousefi, M, Dinarvand, S, Eftekhari Yazdi, M & Pop, I 2018, 'Stagnation-point flow of an aqueous titania-copper hybrid nanofluid toward a wavy cylinder', *International Journal of Numerical Methods for Heat & Fluid Flow*, vol. *28,* no. 7, pp. 1716-1735.